كلية الهندسة بشبرا
FACULTY OF ENGINEERING AT SHOUBRA
ERJ
PRINT ISSN 3009-6049
ONLINE ISSN 3009-6022

ENGINEERING RESEARCH JOURNAL (ERJ)
Volume (54) Issue (1)
January 2025, pp:304-316
https://erjsh.journals.ekb.eg

Performance of Structural Lightweight Reinforced Concrete Solid Slabs with FRP Bars and Contain Polypropylene Fibers

Haytham Emad Diab[1], Yasser A Algash[2], Ahmed N Khater[1]; Ahmed Mahmoud Ahmed[1]
[1] Departmant of Civil Engineering, Faculty of Engineering at Shoubra, Benha university, Cairo, Egypt.
[2] Departmant of Civil Engineering, Aviation and Engineering Technology Institute, Cairo, Egypt
[*] Corresponding Author.
E-mail: haythamdiab95@gmail.com; yaseralgash@iaet.edu.eg; ahmed.khater@feng.bu.edu.eg; ahmed.ahmed@feng.bu.edu.eg.

Abstract: The high cost and limited availability of steel reinforcement within trade fairs, particularly for required diameters and quantities, have become significant challenges. Additionally, reinforcing steel bars corrode rapidly when exposed to the harsh conditions of sustainable infrastructure and marine structures. Given that normal concrete has a density of 2400 kg/m³, it results in high dead weights for structural elements and exhibits low tensile strength. The primary straining action faced by reinforced concrete solid slabs is the bending moment. To enhance the flexural strength of these structural solid slab elements, one effective approach is to reduce the dead weight using lightweight concrete, which has a density range of 300 to 1900 kg/m³. This method also increases the tensile strength of the concrete. Incorporating polypropylene fiber (PPF) into the admixture enhances energy absorption capacity and controls crack propagation. Furthermore, substituting reinforcing steel bars with Glass Fiber Reinforced Polymer (GFRP) bars, which possess high ultimate strength and are non-corrosive, provides significant benefits. This paper aims to experimentally, numerically, and analytically study the impact of PPF on the behavior of lightweight foamed concrete slabs (LWFC) reinforced by GFRP bars. This comprehensive research also explores the mechanisms to improve the mechanical properties of concrete. Key parameters affecting structural behavior addressed in the study include (1) fiber content, (2) type of reinforcement (steel vs. GFRP). The paper utilizes the ABAQUS nonlinear structural program for a numerical finite element analysis to predict the ultimate load. Additionally, an analytical study was conducted to calculate the solid slabs' ultimate loads using code provisions for modeling the equivalent stress block for fibrous concrete in both tension and compression. The findings reveal that using lightweight concrete and GFRP bars increases the flexural strength of solid slabs. Moreover, the inclusion of PPF volume and aspect ratio further improves mechanical properties and controls crack propagation.

Keywords: Solid slabs; fibrous lightweight concrete; Polypropylene fiber; GFRP bars; Numerical analysis; experimental numerical and analytical study.

HIGHLIGHTS

- Studying the effect of using polypropylene fiber (fiber content, fiber aspect ratio) in lightweight concrete on the performance of solid slab;
- Studying the effect of using GFRP bars and steel as reinforcement in solid slabs by changing the reinforcement ratio of the GFRP bars;
- Study some of the variables that affect the behavior of lightweight concrete such as fiber content, fiber aspect ratio and ratio of GFRP reinforcement,

- Comparison between the experimental results with the results from the nonlinear analysis using the ABAQUS program and the analytical results from the international code provisions.

1. INTRODUCTION

Lightweight concrete can define as a type of concrete which include an expanding agent in that, it increases the volume of the mixture while giving additional quantities such as lessened the dead weight [1]. Lightweight concrete was first introduced by the Romans in the second century where "the pantheon " has been constructed using pumice which was the most common type of aggregate used in that particular time [2]. Many experimental studies were performed to point the mechanical properties of reinforced concrete light weight [3]. lightweight concrete has more than excellent thermal and sound insulating properties, noncombustible and cost saving through construction speed and ease of handling. Lightweight concrete has a low tensile strength; therefore, fibers are used to compensate for LWC. Polypropylene fiber can increase structural strength, ductility and reduce crack widths, and tightly control crack widths [4-7]. Polypropylene fiber (PPF) is a new generation chemical fiber. It is manufactured in large scale and have fourth largest volume in production after polyesters, polyamides and a critic. Fibers made and developed using textile and petrochemical industries mono filament of PPF made through an extrusion process. The manufactured PPF is an artificial and thermoplastic product containing various properties of high strength, enhance the durability, low modulus of elasticity, excellent ductility and low price [8]. fibrous light weight concrete is used for construction purpose such as curtain walls, composite flooring systems [9].

Although fibrous concretes have advantage such as polypropylene fiber as a light material but it can cause separation in mixing and impact in mechanical properties of the light weight due to segregation of EPS. Many experiments have been done to avoid separation and one of these experiences is the crushed waste fiber, clay and cement were mixed with water then shape into cake and then dried for 14 days and re crushed into a novel light wight aggregate called SPS [10-11] studies the laboratory assessment of some structural properties of foamed aerated concrete, the properties examined are density, compressive strength and water absorption capacity. The results show that as the ratio of foam concentrate increased the density and compressive strength of test specimens decreased and with increase in curing age there was decrease in density of all test specimens in air. However, with increase in curing age, the average density of specimen cured in water increased which their average compressive strength decreased. Generally, the compressive strength of air cured specimens was higher than the compressive strengths of water- cured test specimens (tasted in saturated state) the absorption capacity test revealed that as the ratio of foam concentrate in the mix increased, the absorption capacity of the aerated concrete decreased. The effect of polypropylene fiber on the behavior of lightweight concrete and the addition of PPF showed a better effect on the concrete tensile strength [7]. The properties of fibers reinforced concrete are affected by type of fiber, shape of fiber, modulus of elasticity of fiber, fiber content, bond strength between fiber and concrete and length of fiber [12]. The ductility of fiber reinforced LWC depends on the ability of fibers to bridge cracks at high level of strain. Addition of PPF decrease the unit weight of concrete and increase its strength of primary role of the PPF in LWC to modify the cracking mechanism by modifying the cracking mechanism where the macro-cracking becomes micro-cracking. The width of these cracks is smaller which reduces the permeability of these cracks is smaller which reduces cracking strain of concrete where fibers are capable of carrying loads across the crack. The stress- strain curve of concrete depends on fiber type, volume and aspect ratio [13-14]. Fiber addition has significant control on the failure modes of concrete and random orientation of fibers improve the fracture properties of concrete, [15]. A study was made where polypropylene was added to concrete with proportions 0.0 to 2.0 kg/m3 and water-cement ratio (W/C) equals 0.48. The results showed that the higher the volume ratio of polypropylene, the higher the compressive strength. The largest strength values were observed at 1.5 kg/m3 and 2 kg/m3 volume ratios [16]. The anisotropic behavior of FRP composites can be characterized by high tensile strength with no yielding only in the direction of the reinforcing fibers. The use of FRP system is governed by a number of considerations related to design requirements, acceptance criteria of FRP material, nature and scope of application in the construction fields. The use of concrete flexural members reinforced with FRP bars are limited only to the use of FRP as tension reinforcement for flexural member such as beams and slabs, as well as shear reinforcement for beams. Consequently, the use of FRP materials as an alternative shear reinforcement in reinforced concrete structures is becoming a more conventional counter measure in structural members subjected to harsh environmental exposure. The design philosophy of the concrete code ECP 203 [17] however, due to brittle failure mode of both FRP bars and concrete, the brittle mode of flexural element will always be brittle. According, the material resistance reduction factor for concrete shall be raised above the usual level of the ductile failure mode as specified. Glass fibres are basically made by mixing silica sand, limestone, folic acid and other minor ingredients. The mix is heated until it melts at about 1260°C. The molten glass is then allowed to flow through fine holes in a platinum plate. finite element analysis is used to confirm the results of the experimental program through ABAQUS program to represent the experimentally tested slabs, and the results from ABAQUS were compared to the experimental ones. The structural elements and material properties used to represent LWC, reinforced steel bars, GFRP bars and steel plates are based on the technical manual of ABAQUS software. A correlative study based on load-deflection curves were adopted to verify the numerical model with the experimental results. Comparative analysis was conducted between the experimental, numerical results, and calculations based on the ECP 208-2019 and ACI 4401R15 codes [18-19]. This comprehensive approach demonstrates the feasibility and benefits of employing various modeling methods for concrete structures, contributing valuable insights into the field.

2. EXPERIMENTAL PROGRAM

2.1 Description of tested specimens

The experimental program features three groups, each consisting of two slabs and a control specimen, as shown in Table 1. Control specimens S1, S2, and S3 are reinforced with different materials. S1 uses a 7 F 10/m' bottom steel mesh without polypropylene fiber. S2 incorporates a 7 F 10/m' bottom GFRP mesh fiber. S3 combines a 7 F 10/m' bottom GFRP mesh and polypropylene fiber to improve the properties of lightweight concrete. All slabs have dimensions of 1000 x 1000 mm with a thickness of 100 mm and a 15 mm concrete cover. Figures 1 and 2 provide detailed slab and reinforcement specifications. The study aims to assess how various reinforcement techniques and materials affect the structural performance of lightweight concrete.

Table 1. Experimental program.

Group	Symbol No.	Studied parameters			Notes
		$\mu/\mu_{balanced}$	Fiber content %	Fiber aspect ratio	
Control specimens	S1	1.4	0.00	0	Control specimen without fiber and reinforced by steel reinforcement
	S2	1.4	0.00	0	Control specimen without fiber and reinforced by GFRP bars
	S3	1.4	0.10	80	Control specimen with fiber and reinforced by GFRP bars
Group 1	S1	1.4	0.00	0	Effect of main reinforcement type
	S2	1.4	0.00	0	
Group 2	S2	1.4	0.00	0	Effect of use of fiber
	S3	1.4	0.10	80	
Group 3	S3	1.4	0.10	80	Effect of GFRP main reinforcement ratio
	S4	1.6	0.10	80	
	S5	1.8	0.10	80	

Table 2. Concrete mix design.

Material	Portland cement	Fine Aggregate (Sand)	Coarse aggregate (Crashed stone)	Sika air	Silica fume	Foam	Superplasticizers	Water	total
	kg	kg	kg	kg	kg	kg	kg	kg	kg
Weight	450	400	510	0.75	50	21	5	185	1621.75

Table 3. Mechanical properties of concrete.

Slab No.	Cubic compressive strength (FCU) MPa	Cylinder compressive strength (f_c`) MPa	Tensile strength (f_t) MPa	Young's modulus (E) MPa
S1	30.00	25.50	3.39	17447
S2	30.00	25.50	3.39	17447
S3	30.26	25.72	3.41	17522

S4	30.26	25.72	3.41	17522
S5	30.26	25.72	3.41	17522
Average	30.16	25.63	3.40	17492
Standard Deviation	0.14	0.12	0.01	41.08

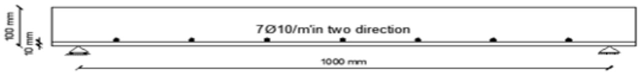

Fig. 1. Cross-section elevation of the tested slabs

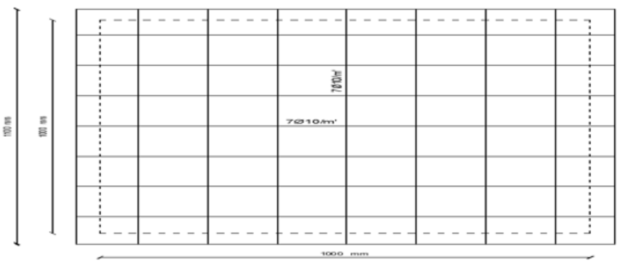

Fig. 2. Reinforcement details of the tested slab in the plan.

2.2 Mixture composition and materials properties

Table 2 details the materials used for the LWC mix for one cubic meter. Experimental tests were conducted to identify their mechanical properties. Twelve concrete cylinders were prepared (150 mm diameter, 300 mm height) and six concrete cubes (150*150*150 mm) for testing. The cubes determined the compressive strength (fcu), while the cylinders assessed the cylindrical compressive strength (fc`) and plotted stress-strain curves. This helped identify the strain at maximum compressive strength ($\varepsilon0$) and elastic modulus per ASTM standards [20-24]. Six additional cylinders were used to determine tensile strength. Average values were 30.16 MPa (fcu), 25.63 MPa (fc`), and 3.40 MPa.

2.3 Characteristics of Materials

The fine aggregate was clean and almost free from impurities with specific gravity 2.63. Crushed hard dolomite size number 1 from Suez Mountain was used as coarse aggregate with specific gravity 2.65. The maximum aggregate size used is 13.2 mm. The nominal size was chosen to account for the cross-section dimensions of the tested slabs as well as the spacing between the reinforcing bars to satisfy the required concrete strength.

Foam used in this research has diameter 1.2mm with specific gravity 0.07 kg/liter. Foam processor was used in mix design us one of the most important features to mountain the resistance and compressive strength for long period because it doesn't leak the gases of concrete. Sika air meets the requirements of ASTM C-260 for air entraining admixtures.

Place ability and workability are improved by the lubricating action of the microscopic bubbles in concrete. Silica fume is a highly effective pozzolanic material, silica fume was used in concrete to improve its material properties like bond strength, compressive strength and reduce permeability, abrasion resistance and therefore helps in protecting reinforcing steel from corrosion because silica fume reacts with the free calcium hydroxides in the mix. Cement used in this investigation was ordinary Portland cement (OPC) CEM I 52.5 N manufactured locally and complies with the Egyptian code ECP 203-2017. High range water reducing super plasticizers is a powerful water reducing agent. It makes the possible to produce fluid concrete with at least 20 mm slump, easily flowing but at the same time free foam segregation and heaving the same W/C ratio as that of a low slump concrete 25mm without admixture. Clean drinking fresh water free from impurities was used for mixing the concrete. The water cement ratio used was chosen based on the total weight of water added to the air-dried material, as no allowance had been made for the absorption of mixing water by the aggregates. Pure polypropylene fiber (CMB fiber) having white color was used in the experimental program with density of 910 Kg/m³. Bundle thickness of 2mm, bundle of fibrils 10, 370 MPa tensile strength and 3750 MPa elastic modulus. Polypropylene fiber used in all specimen.

2.4 Test setup, instrumentations, and test procedure

Recently, an essential experiment was conducted to measure deformations and applied vertical loads on specimen. An external measuring apparatus, specifically Linear Variable Differential Transducers (LVDT), was attached at the mid-span, as noted in Figure 6. Both the load cell and LVDT were connected to a data logger system for precise recording throughout the test stages. Calibration of the load cell and LVDT to zero was performed to meet laboratory standards. To prevent local crushing of Light Weight Concrete (LWC), we used a 200x200x20 mm steel plate and a hydraulic compression machine (1000 kN capacity) to apply the load.

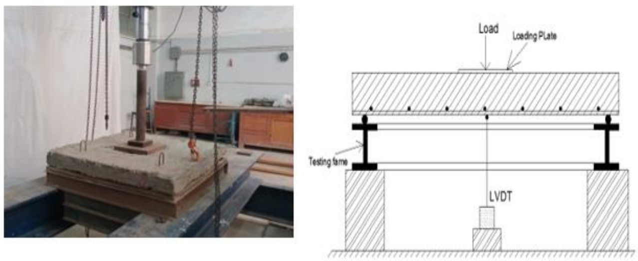

Fig. 3. Test setup and instrumentations.5

3. ANALYSIS OF THE EXPERIMENTAL RESULTS

The results provide valuable insights. Key aspects measured include deflection at mid-span at both the first crack and failure load stages, the load at which the first crack appears, the pattern and distribution of cracks, ultimate failure loads, observed failure modes, secant stiffness values, and specimen toughness. All of the findings were meticulously documented, with a particular focus on comparing these results with those for specimen S3. Detailed data and comparative analysis are available in Tables 4 and 5, aiding us in understanding performance differences among the specimens.

Table 4. Experimental results.

Slab No.	P_{cr} kN	Δcr mm	P_f kN	Δ_f mm	S.S kN/mm	T kN.mm
S1	18.18	1.23	93.24	13.30	7.01	668.73
S2	19.29	0.87	107.16	26.54	4.04	1884.33
S3	25.72	1.06	128.55	26.80	4.80	2259.44
S4	30.82	0.63	154.08	31.41	4.91	3425.39
S5	35.05	0.46	175.26	33.27	5.27	4126.62

Table 5. Experimental results compared to that of specimen S3.

Slab No.	***Pcr/Pcr S3%***	***Pf/Pf S3%***	***Δ_f/Δ_f S3%***	**S.S/S.S S3%**	**T/T S3%**	**Failure Mode**
S1	70.68	72.53	49.63	146.15	29.60	Flexural
S2	75.00	83.36	99.03	84.18	83.40	Flexural
S3	100.00	100.00	100.00	100.00	100.00	Flexural
S4	119.83	119.86	117.20	102.27	151.60	Flexural
S5	136.28	136.34	124.14	109.82	182.64	Flexural

3.1 Load-deflection curves

The experimental load-deflection curves for the nine specimens are plotted in Fig. 4. After reaching the failure load, the load decreases but the deflection increases. Secant stiffness is calculated from the load-deflection curves which showed in Table 5. There was a significant improvement in deflection and failure load recorded for slabs with GFRP bars and PPF. The use of GFRP bars instead of reinforcement steel bars increased the failure load as shown in group 1. By increasing the reinforcement ratio of GFRP bars, the failure mode is compression failure. It can be found that toughness and failure load increased as shown for group 3.

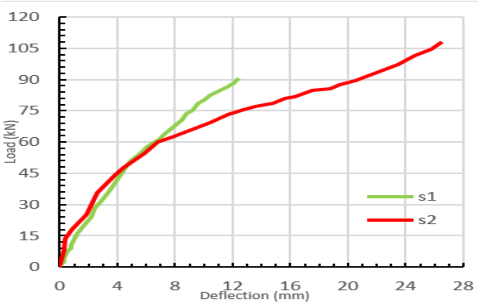

(a)Group 1.

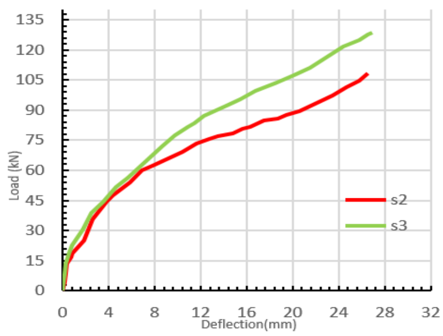

(b)Group 2.

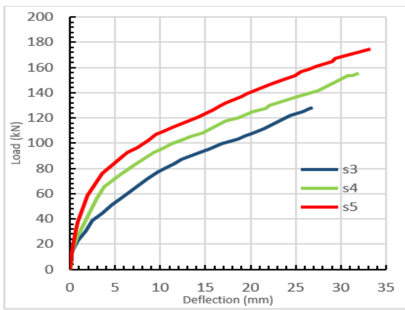

(c)Group 3

Fig. 4. Experimental load-deflection curves for the tested specimens.

3.2 First crack load and cracks pattern

In this study, it was observed consistent crack patterns across all specimens before reaching failure load. Cracks initiated around the loading plate on the tension side at the slab bottom and extended outward. For specimens S1 and S2, S3 cracks emerged at 18 kN, 19.3 kN and 25.72 kN respectively. Overall, PPF addition enhanced first crack load by increasing ductility in Lightweight Concrete. The first crack appears as hair crack at bottom cracks propagated as shown in Fig. 5 tile failure. The first crack load of group 3 increased by 19% compared to specimen S3. The crack load for specimen S3 is increased by 33.33% compared to specimen S2 due to the use of PPF. For group 3, the first crack load for specimens S4 and S5 is increased by 19.83% and 36.28 % respectively compared to S3 due to the increased GFRP bars ratio

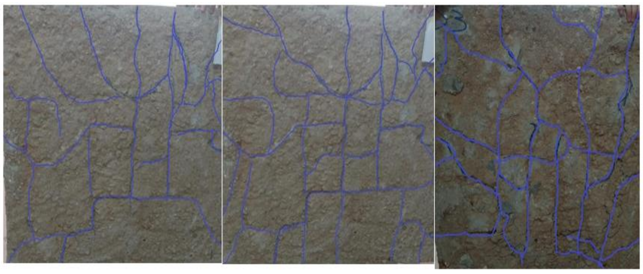

(a) Specimen S1 (b) Specimen S2 (c) Specimen S3

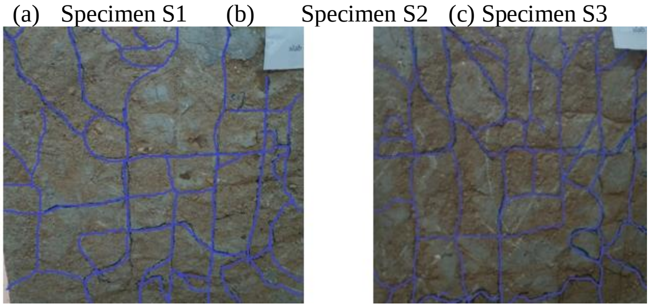

(d) Specimen S4 (e) Specimen S4

Fig. 5. Experimental crack patterns.

3.3 Failure modes

All specimens failed in flexural failure mode as flexural stress is conservative straining action for a two-way solid slab.

3.4 Failure load

In general, there is an increase in the failure load for all specimens has different variables compared to the failure load of the control specimen S3. For group 2 the failure load increases due to the use of PPF in LWC as shown for specimen S3 where the failure load is increased by 17% of the failure load of specimen S2. In group 3, it can be noted that the failure load increased for specimens S4 and S5 by 19% and 36% respectively compared to specimen S3 due to the increase in GFRP reinforcement ratio.

3.5 Secant stiffness (S.S)

Utilizing PPF in LWC exhibits an improvement in the secant stiffness of the slabs as shown in Table 5. The secant stiffness is enhanced for specimens S4, S5 by 2% and 9% respectively compared to specimen S3 due to an increase of GFRP reinforcement ratio compared to specimen S3. Specimen S1 has the largest secant stiffness as the use of steel reinforcement bars gives more ductility and energy absorption capacity than specimens reinforced by GFRP bars.

3.6 Toughness (T)

Toughness (T) is the ability of the specimen to absorb deformations up to the failure load which equals the area under the load-deflection curve up to the failure load (kN.mm). Toughness is a good indication to measure the ductility of the slabs Therefore, it's a function of the failure load P_f and the corresponding deflection Δ_f as shown in Table 5. The result shows that the toughness increased for specimens S4, S5 by 51% and 82 % respectively compared to specimens S3. Toughness for specimens S1 and S2 are 29%, and 83% compared to control specimen S3.

4. NUMERICAL ANALYSIS

1.1 General

A nonlinear finite element analysis was conducted using "ABAQUS" to model and verify structural elements and material properties for lightweight concrete, reinforcement steel bars, GFRP bars, and steel plates. Material properties were derived from the ABAQUS technical manual. A correlative study was performed to validate the numerical model by comparing its load-deflection response with experimental results. This ensured the accuracy and reliability of the model for further analysis and practical applications.

1.1.1 Element types

Utilizing ABAQUS software's diverse finite element library is vital for accurate simulations. For modelling the lightweight concrete slab and steel loading plate, the eight-nodded solid element C3D8R with reduced integration was selected. Longitudinal GFRP and steel bars were represented using the two-nodded linear truss element T3D2. These choices ensure the simulation mirrors real-world behavior, enhancing accuracy and reliability in findings. Emphasizing the importance of selecting appropriate finite elements is crucial for achieving dependable simulation results in both studies and practical applications.

1.1.2 Assembly of element parts

In "ABAQUS", each element of slabs (LWC, GFRP bars, steel bars, and loading steel plates) is built independently in its local coordinates systems. Therefore, it is necessary to use assembly functions to assemble discrete components to form a complete model, as shown in Fig. 6**.**

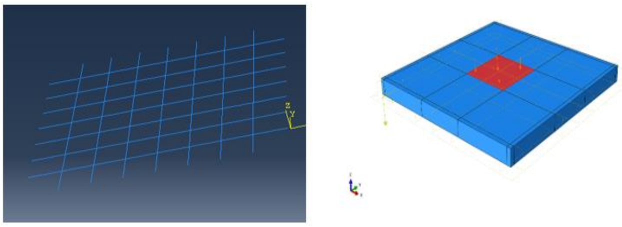

Fig. 6 GFRP and steel bars and assembly parts of concrete slab and loading steel plate

1.2 Verification of the numerical model

Analysis of the numerical simulation results of GFRP-reinforced LWC slabs using various models. The load-deflection curves from these simulations closely matched experimental results, with promising alignment from initial load to failure. Notably, the crack patterns were consistent between numerical models and experiments, affirming the robustness of the simulations. The study also emphasizes the reliability of "ABAQUS" software in accurately simulating LWC slab behavior

Table 6. Comparison between experimental and numerical results.

Slab No.	Experimental $P_{f\ Exp.}$ kN	$\Delta_{f\ Exp.}$ mm	Numerical $P_{u\ Num.}$ kN	$\Delta_{u\ Num.}$ mm	$P_{f\ Exp.}/P_{u\ Num.}$	$\Delta_{f\ Exp.}/\Delta_{u\ Num.}$
S1	90.54	12.40	93.25	13.32	0.97	0.93
S2	108.13	26.49	107.16	26.54	1.00	0.99
S3	128.38	26.88	128.54	26.80	0.99	1.00
S4	155.26	31.98	154.08	31.41	1.01	1.02
S5	174.56	33.27	175.26	33.27	0.99	1.00
Average	-	-	-	-	0.99	0.99
Standard dev.	-	-	-	-	0.01	0.03

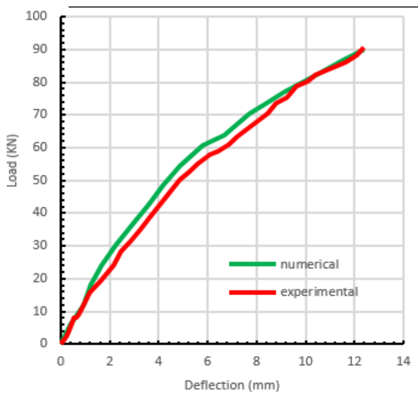

Specimen (S1)

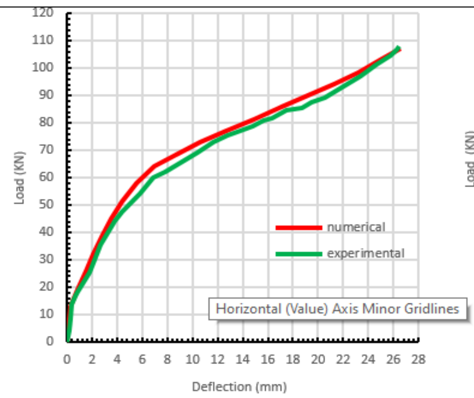

Specimen (S2)

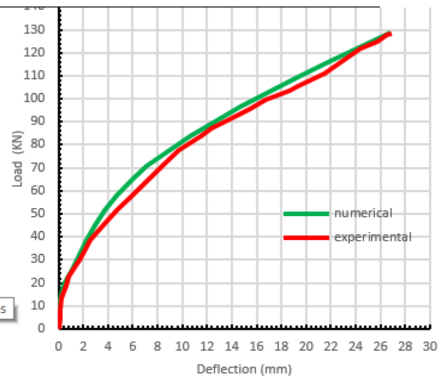

Specimen (S3)

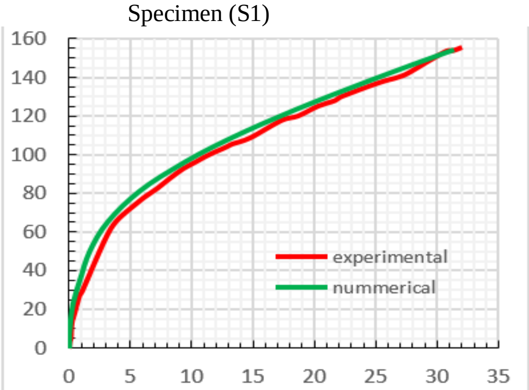

Specimen (S4)

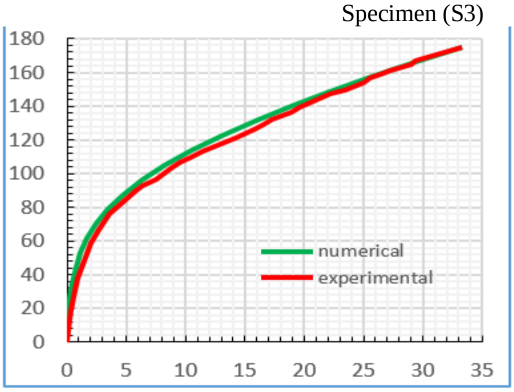

Specimen (S5)

Fig. 7. Experimental and numerical load-deflection curves.

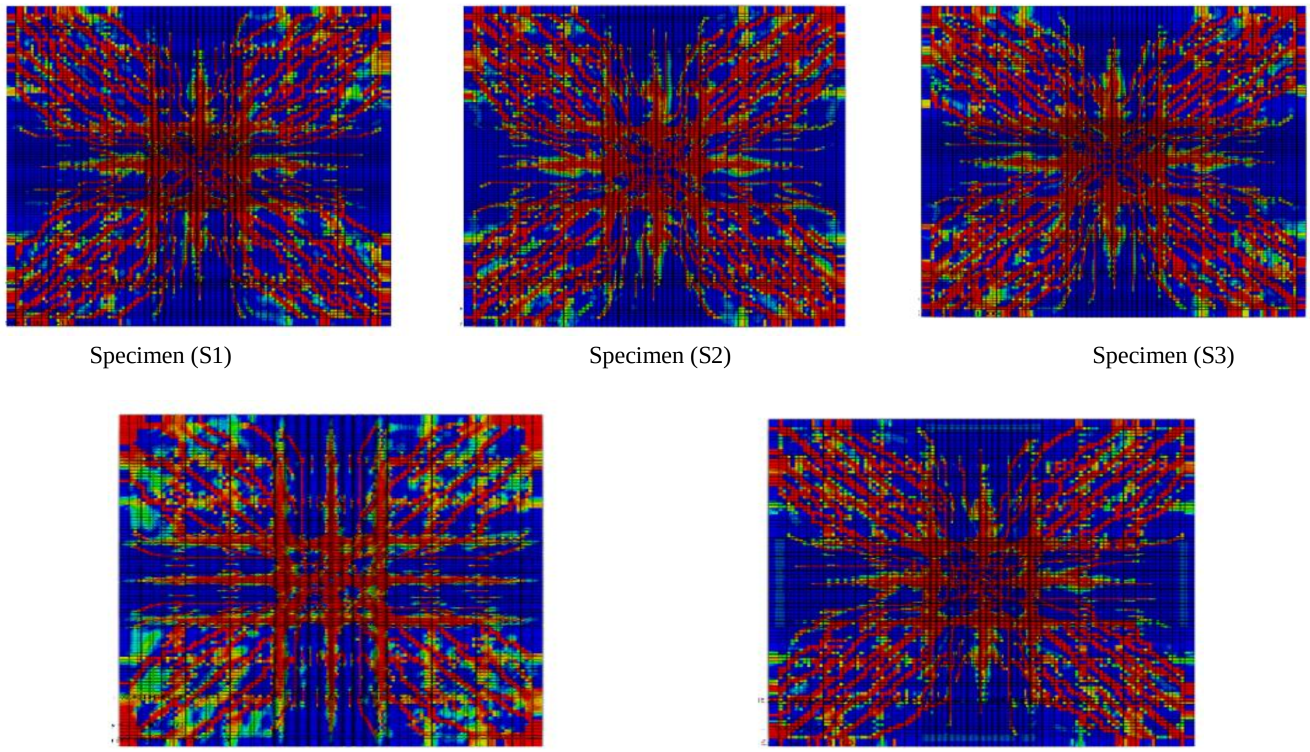

Specimen (S1) Specimen (S2) Specimen (S3)

Specimen (S4) Specimen (S5)

Fig. 8. Numerical crack pattern for the tested specimens.

Table 7. Parametric program.

Studied parameters										
Group No.	Symbol	f_{cu} (MPa)	f_{FRP} (MPa)	μ/μbalanced (-)	t/L (-)	d'/ t (-)	Loading type	Fiber content %	Fiber aspect ratio	Effect of
-	S1	30	1100	1.4	0.1	0.1	Uniform load	0.1	80	Control specimen with fiber
Group 1	S1	30	1100	1.4	0.1	0.1	Uniform load	0.1	80	Fiber content
	S2	30	1100	1.4	0.1	0.1	Uniform load	0.2	80	
	S3	30	1100	1.4	0.1	0.1	Uniform load	0.3	80	
Group 2	S1	30	1100	1.4	0.1	0.1	Uniform load	0.1	80	Fiber Aspect Ratio
	S4	30	1000	1.4	0.1	0.1	Uniform load	0.1	120	
	S5	30	1000	1.4	0.1	0.1	Uniform load	0.1	160	

Table 8. Numerical results.

Slab No.	P_{cr} kN	Δcr mm	P_u kN	Δ_u mm	S.S kN/mm	T kN.mm
S1	55.98	0.77	254.36	21.07	12.07	3888.54
S2	58.28	0.77	264.84	21.12	12.54	4031.80
S3	60.63	0.77	275.57	21.51	12.81	4291.60
S4	57.60	0.77	261.75	21.13	12.39	3993.67
S5	59.13	0.77	268.70	21.12	12.72	4090.52

Table 9. Numerical results compared to specimen S1.

Slab No.	$P_{cr}/P_{cr\ S2}$%	$P_u/P_{u\ S2}$%	$\Delta_u/\Delta_{u\ S2}$%	S.S/S.S S1%	T/T $_{S2}$%	Failure Mode
S1	100.00	100.00	100.00	100.00	100.00	Flexural
S2	104.11	104.12	100.24	103.89	103.68	Flexural
S3	108.31	108.34	102.09	106.13	110.37	Flexural
S4	102.89	102.91	100.28	102.65	102.70	Flexural
S5	105.63	105.64	100.23	105.39	105.19	Flexural

2. PARAMETRIC STUDY PROGRAM

5.1 Details of studies slabs

The experimental tests take a long time and are expensive so they turned to use various methods of modeling LWC slabs using both numerical and analytical models [25-27]. The finite element was used to build the models to study 5 specimens with dimensions 1000*1000 mm, which were divided into 9 groups. The material property for each slab and the effects of some parameters are shown in Table 7.

5.2Analysis of numerical results

The load-deflection curve in Figure 7 highlights the behavior of slabs. Numerical results for all specimens are detailed and compared to specimen S2 in Tables 8 and 9. These tables present crucial response parameters such as first crack load, failure load, secant stiffness, toughness, failure mode, and deflection at the midpoint at various loads, as well as crack patterns depicted in Figure 10. This comprehensive analysis aids in understanding the performance and durability of slabs under different loading conditions

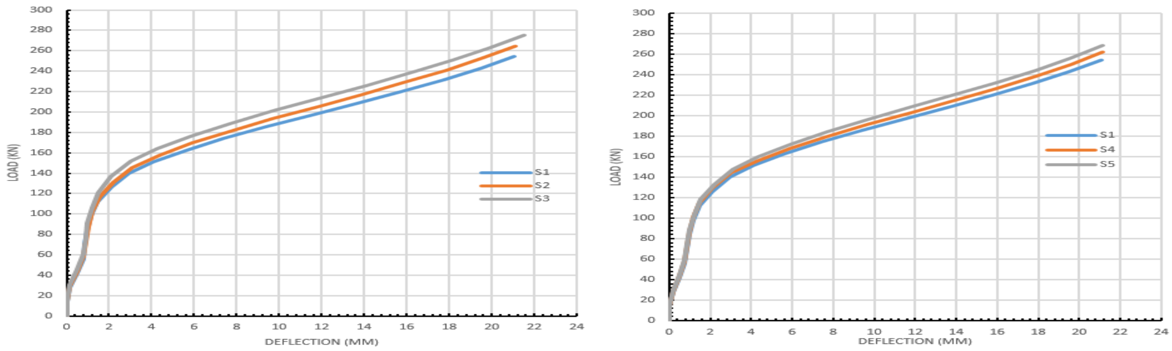

Group (1) Group (2)

Fig.9. Numerical load-deflection curves for the parametric study.

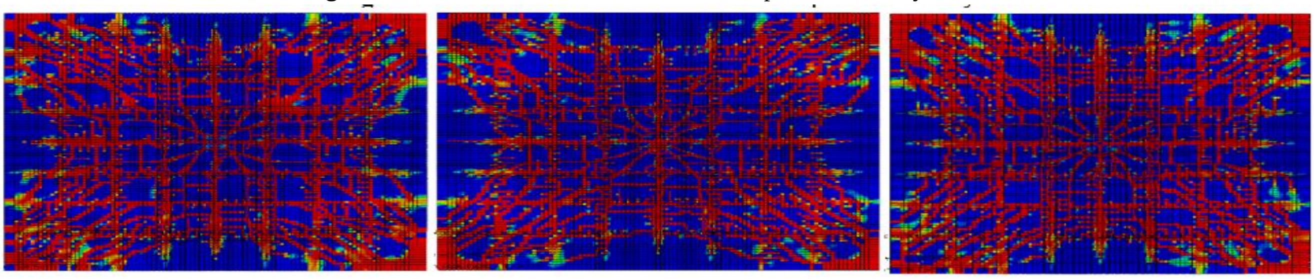

Specimen (S1) Specimen (S2) Specimen (S3)

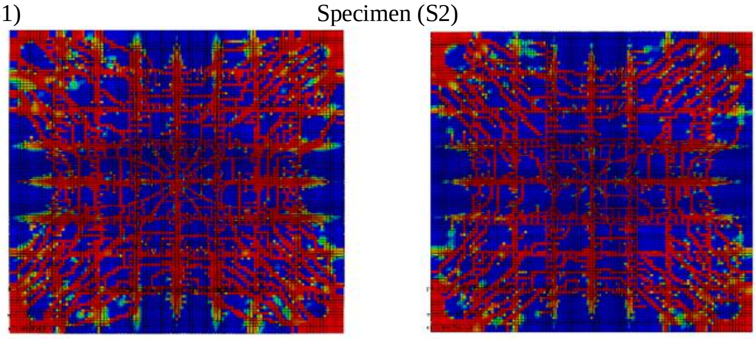

Specimen (S4) Specimen (S5)

Fig. 10. Numerical cracks pattern for the parametric study.

5.3 Effect of the fiber content

The effect of polypropylene fiber content in LWC slabs are shown in Table 8, (group 1) for specimens S1, S2, and S3 containing different fiber content percentage of 0.1%, 0.2%, and 0.3% respectively. As shown in Fig. 9, the load-deflection curves for each specimen show different results. The ultimate load for specimens S2, and S3 increased by 4% and 8% respectively compared to specimen S1. Secant stiffness for specimens S2 and S3 increased by 3% and 6% respectively compared to specimen S1. Toughness for specimens S2, and S3 increased by 3% and 10% respectively compared to specimen S1. The increase of fiber content in LWC slabs increases the ultimate load capacity for, toughness and secant stiffness.

5.4 Effect of fiber aspect ratio

The fiber aspect ratio is the length of the fiber divided by its diameter. Three specimens S1, S4, and S5 (group 2) with varying aspect ratios of 80, 120, and 160 respectively were used to study this factor as shown in Table 8. The load-deflection curves for group 2 show varying results for each specimen as shown in Fig. 9. The ultimate load capacity for specimens S4 and S5 increased by 2.91% and 5.64% respectively compared to specimen S1. Secant stiffness for specimens S4 and S5 increased by 2.65% and 5.39% respectively compared to specimen S1. Toughness for specimens S4 and S5 increased by 2.7% and 5.19% respectively compared to specimen S1. The increase of fiber aspect ratio in LWC slabs increases the ultimate load capacity, toughness, and secant stiffness.

6.0 PROPOSED DESIGN EQUATIONS

6.1 Based on ECP 208-2019 [18]

The stress-strain distribution for RC slabs cross section based on ECP 208-2019 [18] is shown in Fig.18. Equations 1 through 6 are used to calculate the nominal flexural strength M_n of PPF lightweight concrete from which $P_{u\ ECP}$ [18] can be calculated as shown in Table 11.

$$f_{cuf} = f_{cu}*(1+0.1066* V_f* (L_f/ø)) \quad (1)$$

$$f_{pp}= 1.64* V_f* (L_f/ø) \quad (2)$$

$$CC= T_f + T_{pp} \quad (3)$$

$$0.67*\frac{fcuf}{ɣc}* a*b = A_f * \frac{F*fe}{ɣf}+ f_{pp}* b* (t-c) \quad (4)$$

$$ɣ_c= ɣ_f =1.7 \text{ (as compression failure)} \quad (5)$$

$$M_u = T_f* (d-\frac{a}{2})+ T_{pp} * (t+ c-a)/2 \quad (6)$$

Where:

ε_c: strain in concrete;

ε*fe: design rupture strain of FRP reinforcement;

c : distance from extreme compression fiber to the neutral axis;

t : the thickness of the slab;

M_u: nominal moment capacity;

T_f: tension force of GFRP bars;

T_{op}; tension force of fiber;

d: distance from extreme compression fiber to centroid of tension reinforcement; and

a: depth of equivalent rectangular stress block which is equal to = 0.8c.

6.2 Based on ACI 4401R15 [19]

Utilizing the stress block philosophy, the nominal flexural strength M_n of lightweight concrete based on ACI 4401R15 [19] code can be calculated from Equations 10 through 12:

$$\sqrt{\frac{(Ef*\varepsilon cu)^2}{4}+\frac{(0.85*B1*fc\prime)}{pf}*Ef*\varepsilon cu}-0.5*Ef*\varepsilon cu] \le f_{fu} \quad (10)$$

$$A_{f\ min} = \frac{0.41*\sqrt{fc\prime}}{fFu}*b*d \ge \frac{2.3}{fFU}*b*d \quad (11)$$

$$M_n= pf*ff*[1-0.59*\frac{pf*ff}{fc'}]*b*d^2 \quad (12)$$

Where:

f_f: stress in GFRP reinforcement;

E_f: design modulus of elasticity of GFRP;

ε_{cu}: ultimate strain in concrete;

f_c' specified compressive strength of concrete;

ρ_f: fiber-reinforced polymer reinforcement ratio;

f_{fu}: design tensile strength of FRP, defined as the guaranteed tensile strength; multiplied by the environmental reduction factor;

$A_{f\ min}$: minimum area of GFRP reinforcement needed to prevent failure of flexural members upon cracking; and

b: width of the slab cross-section

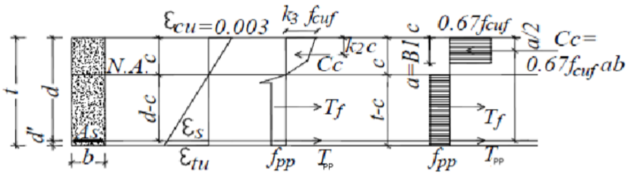

Fig. 11. Stress-strain distribution for RC cross-section.

Where B1: factor is taken as 0.85 for concrete strength fc' up to 28 MPa. For strength above 28 MPa, this factor is reduced continuously at a rate of 0.05 per every 7 MPa of strength over 28 MPa but isn't taken less than 0.65.

6.3 Comparison of results

The numerical results were compared with those calculated from ECP 208-2019 [18] and ACI 4401R15 [19] as shown in Table 10. In comparison to the code provisions, the ACI-318-2019 code achieved superior analytical results with a mean predicted-to-analytical failure load ratio of 0.98, with 0.04 standard deviation while the ECP-203-2019 code produced fewer conservative results with analytical -to- predicted failure load with average value 0.95 and standard deviation 0.08. Therefore, both the ACI-318-2019 code and ECP-203-2019 code is conservative and the ECP-203-2019 code is most conservative.

Table 10. Comparison between numerical, and analytical results from ECP [18] and ACI [19] codes.

Slab No.	P_u (ECP) (kN)	$P_{u(}$ ACI) (kN)	P_u (ECP)/ P_u (Numerical) (-)	P_u (ACI)/ P_u (Numerical) (-)	P_u (ECP)/ P_u (ACI) (-)
S1	253.37	255.06	1.00	1.00	0.99
S2	248.65	256.35	0.94	0.97	0.97
S3	246.00	257.63	0.89	0.93	0.95
S4	250.00	255.71	0.96	0.98	0.98
S5	248.65	256.35	0.93	0.95	0.97
Average	-		0.94	0.97	0.97
Standard Deviation	-		0.04	0.02	0.01

7. CONCLUSIONS

For the range of the studied parameters, the following conclusions can be drawn:

1- Polypropylene fiber is added to LWC, it's founded an improvement of the structural properties, particularly tensile and flexural strength, ultimate load capacity and the extent of improvement in the mechanical properties achieved with PPF over those of plain concrete depends on several factors such as shape, size, volume fraction (percentage) and distribution type of fibers.

2- the increase of fiber aspect ratio in LWC slabs increases the ultimate load capacity, toughness, and secant stiffness.

3- The increase of fiber content in LWC slabs increases the ultimate load capacity for, toughness and secant stiffness.

4- The use of steel reinforcement bars gives more ductility and energy absorption capacity than specimens reinforced by GFRP bars.

5- The increase of the slab GFRP reinforcement ratio increases ultimate load capacity and higher stiffness while decreasing toughness

6- The increase of polypropylene fiber (PPF) properties such as fiber content or aspect ratio in LWC results in an increase in energy absorption capacity and secant stiffness. A high aspect ratio provides more effective post-peak performance because of their increase in resistance of pullout from LWC.

7- The use of glass-reinforced polymers (GFRP) bars increases the loading capacity and toughness of slabs compared to the reinforcement steel bars while decreasing the secant stiffness and ductility due to their brittle failure.

8- Nonlinear analysis using the ABAQUS program can perfectly represent LWC solid slabs to a good extent, where the average and standard deviation of numerical to experimental results are 1.0 and 0.02 respectively.

REFERENCES

[1] Kamsia.M.I," study of light weight concrete behavior " technology university Malaysia institutional Repository ,2003,4567. https://www.researchgate.net/publication/311232955_Behavioural_Study_on_Lightweight_Concrete

[2] Abdullahi ,H.M.A and Al-mattareneh ,B.S.M "mix design of structural light weight concrete using developed models" , engineering science and technology,2011, 520-531. https://www.researchgate.net/publication/228747498_m-file_for_mix_design_of_structural_lightweight_concrete_using_developed_models.

[3] Sabaa, B., and Rasiah S. R., "Engineering Properties of Lightweight Concrete Containing Crushed Expanded Polystyrene Waste", Proceedings of the Symposium MM: Advances in Materials for Cementitious Composites, Boston, MA, USA. 1997,1-3. https://www.researchgate.net/publication/265916085_Engineering_properties_of_lightweight_concrete_containing_crushed_expanded_polystyrene_waste

[4] E. G. Badogiannis, K. I. Christidis, and G. E. Tzanetatos, Evaluation of the mechanical behavior of pumice lightweight concrete reinforced with steel and polypropylene fibers, Construction and Building Materials, 2019 (196) 443-456. https://www.researchgate.net/publication/329155406_Evaluation_of_the_mechanical_behavior_of_pumice_lightweight_concrete_reinforced_with_steel_and_polypropylene_fibers

[5] S. Mukhopadhyay and A. S. Khatan, A review on the use of fibers in reinforced cementitious concrete, Journal of Industrial Textiles, 2015 (45) 2 (239-264). https://www.researchgate.net/publication/275451853_A_review_on_the_use_of_fibers_in_reinforced_cementitious_concrete.

[6] M. A. Aziz, P. Paramasivam and S. L. Lee, Prospects for natural fiber reinforced concretes in construction, International Journal of Cement Composites and Lightweight Concrete, 1981 (3) 2 (123-132). https://www.researchgate.net/publication/325373849_Flexural_properties_of_reinforced_date_palm_fibres_concrete_in_Sahara_climate.

[7] V. Srinivasu, and N. V. Padmavathi, An experimental investigation on strength properties of polypropylene fibers, IJESRT Journal of Engineering Sciences,2018 (7) 12 (419-436). https://www.researchgate.net/publication/342502249_Experimental_investigation_on_strength_properties_of_poly_-_propylene_fibre_reinforced_concrete

[8] Jianzhuang X., and Falkner, H.," On residual strength of high-performance concrete with and without polypropylene fibers at elevated temperatures", Fire Safety Journal, 41,115–121, 2006. https://www.researchgate.net/publication/222113733_On_residual_strength_of_high-performance_concrete_with_and_without_polypropylene_fibres_at_elevated_temperature.

[9] Chen, B., and Juanyu, L., "Properties of Lightweight Expanded Polystyrene Concrete Reinforced with Steel Fiber", Journal of Cement and Concrete Research, 2004, 34.7: 1259-1263. https://www.researchgate.net/publication/248357473_Properties_of_lightweight_expanded_polystyrene_concrete_reinforced_with_steel_fiber

[10] Herki, B. M. A., and Khatib, J. M., "Structural Behavior of Reinforced Concrete Beams Containing a Novel Lightweight Aggregate", International Journal of Structural Engineering, 2016, 7(1), 1-30. https://www.researchgate.net/publication/288872112_Structural_behaviour_of_reinforced_concrete_beams_containing_a_novel_lightweight_aggregate

[11] F.falade, E.E lkponmwosa and a.arogundade " investigation of some structural properties of foamed aerated concrete", journal of engineering research, vol. 16, No. 1, march 2011. https://www.researchgate.net/publication/360235777_Investigation_the_Properties_of_Foam_Concrete_A_review

[12] Aziz, M. A., Paramasivam, P., and Lee, S. L., "Prospects for Natural Fiber Reinforced Concretes in Construction," International Journal of Cement Composites and Lightweight Concrete 3.2, 1981: 3.2: 123-132. https://www.academia.edu/89603958/Prospects_for_natural_fibre_reinforced_concretes_in_construction

[13] Shah, S. P., Stroeven, P., Dalhuison, D., and Steleelenburg, V. P., "Complete Stress-Strain Curves for Steel Fiber-Reinforced Concrete in Uniaxial Tension and Compression", Proceedings of RIEM Symposium on Testing and Test Methods of Fiber Cement Composites, Construction Press, U.K., 1978, 399-408. https://www.researchgate.net/publication/270485440_Stress-strain_curves_for_steel_fiber-reinforced_concrete_in_compression

[14] Bahn, B. Y. and Hsu, C. T. T., "Stress-Strain Behavior of Concrete under Cyclic Loading", ACI Materials" Journal, 1998, 95: 178-193. https://www.concrete.org/publications/internationalconcreteabstractsportal/m/details/id/363.

[15] Thirumurugan, S, and Siva K., A., "Compressive Strength Index of Crimped Polypropylene Fibers in High Strength Cementitious Matrix" World Applied Sciences Journal, 2013, 24 (6), 698-702. https://www.researchgate.net/publication/288405387_Compressive_strength_index_of_crimped_polypropylene_fibres_in_high_strength_cementitious_matrix

[16] Bagherzadeh, R., Abdol, H. S., and Masoud L., "Utilizing Polypropylene Fibers to Improve Physical and Mechanical Properties of Concrete", Textile Research Journal, 2012, 82.1: 88-96. https://www.researchgate.net/publication/258196240_Utilizing_polypropylene_fibers_to_improve_physical_and_mechanical_properties_of_concrete

[17] ECP 203-2020, "Egyptian Code of Practice for Design and Construction of Reinforced Concrete Structures", Housing and Building Research Center, Ministry of Building and Construction, Giza, Egypt, 2020. https://www.scirp.org/reference/referencespapers?referenceid=2649189

[18] Egyptian Code of Practice for the Use of Fiber Reinforced Polymer (FRP) in the Construction Fields ECP-208, Housing and Building Research Center, Ministry of Building and Construction, Giza, Egypt, (2005). https://www.cuipcairo.org/en/directory/housing-building-national-research-center

[19] ACI Committee 440, Guide for the Design and Construction of Structural Concrete Reinforced with Fiber-Reinforced Polymer (FRP) Bars, ACI 4401R15, American Concrete Institute, Farmington Hills, Mirch,2015. https://basalt-fibers.com/wp-content/uploads/2021/05/Standart_ACI-4401R15.pdf

[20] ASTM International, Standard Test Method for Compressive Strength of Cylindrical Concrete Specimens, ASTM C39/ C39M – 14, (2015). https://www.studocu.com/row/document/state-engineering-university-of-armenia/concrete-design/astm-c39-c39m-14-concrete-design/32367366.

[21] ASTM International, Standard Test Method for Static Modulus of Elasticity and Poisson's Ratio of Concrete in Compression, ASTM C469 / C469M-14, West Conshohocken, (2021). https://www.astm.org/c0469_c0469m-14.html.

[22] ASTM International, Standard Test Method for Splitting Tensile Strength of Cylinders Concrete Specimens ASTM C496-96, (2015). https://www.astm.org/c0496-96.html.

[23] ASTM International, Standard Test Methods and Definitions for Mechanical Testing of Steel Products, ASTM, (2017). West Conshohocken, PA. A370-17a. https://www.astm.org/a0370-17.html.

[24] ASTM D7205 Tensile Tests of GFRP Matrix Composite Bars https://www.testresources.net/applications/standards/astm/astm-d7205-tensile-tests-of-gfrp-matrix-composite-bars/#:~:text=ASTM%20D7205%20determines%20the%20quasi,%2C%20or%20post%2Dtensioned%20concrete.

[25] International Federation for Structural Concrete (FIB). FIB model code for concrete structures, Ernst and Sohn, a Wiley Brand, 2013. https://books.google.com.sa/books?id=Xf91AQAAQBAJ&printsec=frontcover&source=gbs_ViewAPI&redir_esc=y#v=onepage&q&f=false.

[26] J. Lubliner, J. Oliver, S. Oller, and E. Oñate, A plastic-damage model for concrete. International Journal Solids and Structures,1989. https://www.scipedia.com/wd/images/b/b7/Lubliner_et_al_1989a_3657_LuOllOliOn1989.pdf.

[27] M. Musmar, Nonlinear finite element flexural analysis of RC beams, International Journal of Applied Engineering Research, 2018(13.4). https://www.researchgate.net/publication/338234438_Nonlinear_Finite_Element_Flexural_Analysis_of_RC_Beams.

Nomenclature

LWC: Light Weight Concrete;

GFRP: Glass Fiber Reinforced Polymer;

PPF: Polypropylene Fiber;

f_{cu}: Cubic concrete characteristic compressive strength after 28 days;

fc': Cylindrical concrete characteristic compressive strength after 28 days;

f_{cuf}: Cubic concrete compressive strength enhanced with fiber after 28 days;

μ: Reinforcement ratio;

V_f: Fiber content percent;
$L_f/ø$: Fiber aspect ratio;
L_f: Fiber length;
Ø: Diameter of fiber;
P_{cr}: First crack load;
P_f: Failure load;
P_u: Ultimate load;
Δ_{cr}, Δ_f: Deflection at first crack load and failure load respectively;
f_{FRP}: Ultimate tensile strength of GFRP bar;
t: Slab thickness;
d': Concrete cover;
S.S: Secant stiffness = P_f/Δ_f; and
T: Toughness, which is equal to the area under the load-deflection curve up to failure.